Dielectric Haloscopes: A New Way to Detect Axion Dark Matter

Allen Caldwell,[1] Gia Dvali,[1,2,3] Béla Majorovits,[1] Alexander Millar,[1] Georg Raffelt,[1] Javier Redondo,[1,4] Olaf Reimann,[1] Frank Simon,[1] and Frank Steffen[1]

(The MADMAX Working Group)

[1] *Max-Planck-Institut für Physik, Föhringer Ring 6, 80805 Munich, Germany*
[2] *Ludwig Maximilians Universität, Theresienstraße 37, 80333 Munich, Germany*
[3] *CCPP, New York University, 10003 New York, USA*
[4] *University of Zaragoza, P. Cerbuna 12, 50009 Zaragoza, Spain*

We propose a new strategy to search for dark matter axions in the mass range of 40–400 μeV by introducing dielectric haloscopes, which consist of dielectric disks placed in a magnetic field. The changing dielectric media cause discontinuities in the axion-induced electric field, leading to the generation of propagating electromagnetic waves to satisfy the continuity requirements at the interfaces. Large-area disks with adjustable distances boost the microwave signal (10–100 GHz) to an observable level and allow one to scan over a broad axion mass range. A sensitivity to QCD axion models is conceivable with 80 disks of 1 m^2 area contained in a 10 Tesla field.

PACS numbers: 14.80.Va, 95.35.+d

INTRODUCTION

The nature of dark matter (DM) is one of the most enduring cosmological mysteries. One prime candidate, the axion, arises from the Peccei–Quinn (PQ) solution to the strong CP problem, the absence of CP violation in quantum chromodynamics (QCD). The CP violating QCD phase θ is effectively replaced by the axion field whose potential is minimal at $\theta = 0$ [1–3]. Thus θ dynamically relaxes towards zero regardless of its initial conditions, satisfying the neutron electric dipole moment constraints $\theta \lesssim 10^{-11}$ [4].

Tiny relic oscillations with a frequency given by the axion mass m_a around $\theta = 0$ persist, acting as cold DM [5–7]. If DM is purely axionic, its local galactic density $\rho_a = (f_a m_a)^2 \theta_0^2/2 \sim 300\,\mathrm{MeV/cm^3}$ implies $\theta \sim \theta_0 \cos(m_a t)$ at the Earth, with $\theta_0 \sim 4\times10^{-19}$. While these oscillations could be detected, the main challenge is to scan over a huge frequency range as m_a is unknown.

However, cosmology can guide our search. Causality implies that at some early time θ is uncorrelated between patches of causal horizon size. We consider two cosmological scenarios depending on whether cosmic inflation happens after (A) or before (B) that time.

In Scenario A, one patch is inflated to encompass our observable universe while smoothing θ to a single initial value θ_I. The cosmic axion abundance depends on both θ_I and m_a, so the DM density can be matched for any m_a allowed by astrophysical bounds [8] for a suitable θ_I.

In Scenario B, the axion abundance is given by the average over random initial conditions and the decay of accompanying cosmic strings and domain walls. Freed from the uncertain initial conditions, Scenario B provides a concrete prediction $m_a \sim 100\,\mu$eV [9, 10], although with some theoretical uncertainty [11].

Searches based on cavity resonators in strong magnetic fields (Sikivie's haloscopes [12]) such as ADMX [13], ADMX HF [14] or CULTASK [15] are optimal for $m_a \lesssim 10\,\mu$eV. Much lower values of m_a can be explored by nuclear magnetic resonance techniques like CASPER [16] or with LC circuits [17, 18].

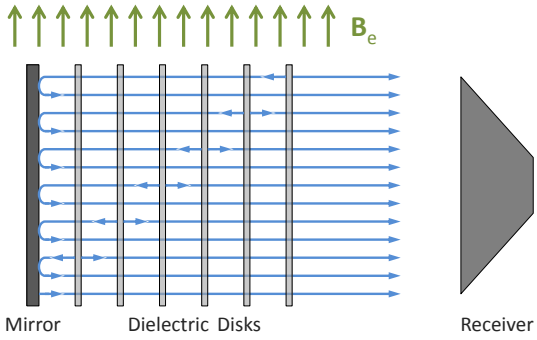

FIG. 1. A dielectric haloscope consisting of a mirror and several dielectric disks placed in an external magnetic field $\mathbf{B}_\mathrm{e}$ and a receiver in the field-free region. A parabolic mirror (not shown) could be used to concentrate the emitted power into the receiver. Internal reflections are not shown.

The mass range favoured in Scenario B is untouched by current experiments, and for cavity haloscopes will remain so for the foreseeable future. While fifth-force experiments [19] could search this region, they would not reveal the nature of DM. We present here a proposal to cover this important gap, capable of discovering $\sim 100\,\mu$eV mass axions. It consists of a series of parallel dielectric disks with a mirror on one side, all within a magnetic field parallel to the surfaces as shown in Fig. 1 – a dielectric haloscope.

For large m_a the greatest hindrance for conventional haloscopes is that the signal is proportional to the volume of the cavity. With dimensions of order of the ax-

ionic Compton wavelength[1] $\lambda_a = 2\pi/m_a$, the volume decreases rapidly with m_a. While there are plans to couple multiple high-quality cavities, use open resonators, or compensate with extremely high magnetic fields and/or new detectors, these techniques may not prove practical for large m_a [15, 22–24].

A radical approach to increase the volume is to use a dish antenna inside a B-field to convert axion DM into electromagnetic (EM) radiation [25]. The resonant enhancement of the axion-photon conversion is given up in favour of a large transverse area $A \gg \lambda_a^2$.

In our dielectric haloscope each disk acts as a flat dish antenna, emitting EM waves. As our dielectrics are partially transparent, the waves emitted by each disk are reflected by and transmitted through the other disks before exiting. With suitable disk placement, these waves add coherently to enhance the emitted power. While the use of $\lambda_a/2$ dielectric layers has been already proposed in the dish antenna [26] and cavity haloscope concepts [23], our disks do not have to be $\lambda_a/2$-thick because the coherence of the emitted waves can be controlled by the disk separations. This allows scans over a band of m_a without needing to use disks with different thicknesses for each measurement.

AXION INDUCED *E*-FIELD

The axion-photon interaction is described by

$$\mathcal{L}_{\rm int} = -\frac{\alpha}{2\pi} C_{a\gamma} \mathbf{E}\cdot\mathbf{B}\,\theta, \tag{1}$$

where $\mathbf{E}$ and $\mathbf{B}$ are electric and magnetic fields, $\theta = \theta(x^\mu) = a(x^\mu)/f_a$ represents the axion field, and $C_{a\gamma} = \mathcal{E}/\mathcal{N} - 1.92$, where $\mathcal{E}$ and $\mathcal{N}$ are the EM and colour anomalies of the PQ symmetry [2], respectively. We are interested in galactic DM axions, which are in a highly occupied state and very non-relativistic ($v_a \lesssim 10^{-3}$). Thus we treat θ as a classical field and take the zero-velocity limit, making it homogeneous $\theta(t) = \theta_0 \cos(m_a t)$ and approximately monochromatic. Homogeneity holds as the typical de Broglie wavelength, $2\pi/m_a v_a \gtrsim 12.4\,\text{m}$ for $m_a = 100\,\mu\text{eV}$, is larger than the dimensions of our dielectric haloscope, a cubic meter. The axion mass $m_a = 57.0\,\mu\text{eV}\,\left(10^{11}\,\text{GeV}/f_a\right)$ [27] is related to the axion decay constant f_a which we will treat as a free parameter.

The interaction (1) enters as a current in the Ampère-Maxwell equation,

$$\nabla\times\mathbf{B} - \epsilon\dot{\mathbf{E}} = \frac{\alpha}{2\pi} C_{a\gamma}\mathbf{B}\,\dot{\theta}, \tag{2}$$

for a medium with permeability $\mu = 1$ and dielectric constant ϵ. When a static and homogeneous magnetic field $\mathbf{B}_{\rm e}$ is applied, the axion DM field sources a tiny electric field,

$$\epsilon\mathbf{E}_a(t) = -\frac{\alpha}{2\pi} C_{a\gamma}\mathbf{B}_{\rm e}\,\theta(t)\,. \tag{3}$$

The induced E-field is discontinuous at the boundary between media of different ϵ. However, the usual continuity requirements, $\mathbf{E}_{\parallel,1} = \mathbf{E}_{\parallel,2}$ and $\mathbf{B}_{\parallel,1} = \mathbf{B}_{\parallel,2}$ (recall $\mu = 1$), still apply. Thus, EM waves of frequency $\nu_a = m_a/2\pi$ must be present. In effect, breaking translational invariance couples the non-propagating axion-induced E-field with propagating waves, which we aim to detect. The EM waves are perpendicular to the surface in our zero-velocity limit [25]. We require flat surfaces of large area to avoid diffraction, $A \gg \lambda_a^2$, so we can work in a 1D framework. For maximum effect, $\mathbf{E}_a$ and thus $\mathbf{B}_{\rm e}$ must be parallel to the interface [25].

The axion field induces plane EM waves for every change of media, which we can arrange to interfere constructively to enhance the amplitude. We define the boost factor [28]

$$\beta(\nu_a) \equiv |E_{\rm out}(\nu_a)/E_0|, \tag{4}$$

to quantify the enhancement in the amplitude of the emitted EM wave, $E_{\rm out}$, with respect to that emitted by a flat dish antenna, a planar perfect mirror into vacuum, $E_0 \equiv \alpha/(2\pi)\,|C_{a\gamma}\mathbf{B}_{\rm e}\,\theta_0|$ [25]. This corresponds to an EM power per unit area [25]

$$\frac{P}{A} = \beta^2\frac{E_0^2}{2} = 2.2\times10^{-27}\,\beta^2\,\frac{\text{W}}{\text{m}^2}\left(\frac{B_{\rm e}}{10\ \text{T}}\right)^2 C_{a\gamma}^2\,. \tag{5}$$

The boost factor can be calculated by matching $\mathbf{E}_a$ in each region (dielectric disk or vacuum) with left and right-moving EM waves to satisfy the continuity of the total $\mathbf{E}_{||}$ and $\mathbf{B}_{||}$ fields. This can be achieved via the transfer matrix formalism [26].

The enhancement comes from two effects, which generally act together but can be differentiated in limiting cases. They depend on the optical thickness of one disk $\delta = 2\pi\nu d\sqrt{\epsilon}$, with d the physical thickness and ν the frequency, which sets the transmission coefficient of a single layer $\mathcal{T} = i2\sqrt{\epsilon}/[i2\sqrt{\epsilon}\cos\delta + (\epsilon+1)\sin\delta]$. When $\delta = \pi, 3\pi, 5\pi, ...$, the disk is transparent, $\mathcal{T} = 0$, and the emission from different disks can be added constructively by placing them at the right distance. When $\mathcal{T} \neq 0$, the spacings can be adjusted to form a series of leaky resonant cavities where E-fields are boosted by coherent reflections between the disks. In general both the simple adding of emitted waves and resonant enhancements are important.

COMPARISON WITH CAVITY HALOSCOPES

More insight is gained by contrasting dielectric haloscopes with resonant cavities. The signal power extracted

[1] We use natural units with $\hbar = c = 1$ and the Lorentz-Heaviside convention $\alpha = e^2/4\pi$.

from a cavity haloscope resonantly excited by axion DM is [29]:

$$P_{\rm cav} = \kappa \mathcal{G} V \frac{Q}{m_a} \rho_a g_{a\gamma}^2 B_{\rm e}^2, \;\; \mathcal{G} = \frac{\left(\int dV \mathbf{E}_{\rm cav} \cdot \mathbf{B}_{\rm e}\right)^2}{V B_{\rm e}^2 \int dV \mathbf{E}_{\rm cav}^2}, \quad (6)$$

where V is the volume, $g_{a\gamma} = -\alpha/(2\pi f_a) C_{a\gamma}$, Q is the loaded quality factor, and κ is the ratio of signal power to total power loss. The form factor $\mathcal{G}$ involves the E-field of the resonant mode, $\mathbf{E}_{\rm cav}(\mathbf{x})$, calculated by imposing closed boundary conditions as a perturbation of the closed system.

Dielectric haloscopes are open systems, which are in general non-resonant. Nevertheless, one can find analogies for the various terms in (6) and so derive a similar expression as shown in a forthcoming paper [28]

$$P \simeq \mathcal{G}_{\rm d} V \frac{Q_{\rm d}}{m_a} \rho_a g_{a\gamma}^2 B_{\rm e}^2, \quad (7a)$$

$$\mathcal{G}_{\rm d} = \frac{\left|\int dx E_{\rm in} B_{\rm e}\right|^2}{L B_{\rm e}^2 \int dx |E_{\rm in}|^2}, \;\; Q_{\rm d} = \frac{1}{4} \frac{\int dx |E_{\rm in}|^2}{E_0^2/m_a}, \quad (7b)$$

where L is the length of the haloscope and $E_{\rm in}(x)$ is the E-field inside the haloscope induced by shining a wave of amplitude E_0 from the RHS in Fig. 1. Notice that $E_{\rm in}(x)$ is not generally a physical mode excited by the axion field, but only a way to encode the boundary conditions at the interfaces. While $\mathcal{G}_{\rm d}$ is a true form factor, note that $Q_{\rm d}$ is not strictly speaking a quality factor. The output coupling is built into our formalism and does not require an additional factor.

Thus our goal is to maximise P by increasing V and $\mathcal{G}_{\rm d}$ using appropriately placed dielectrics. This is similar to enhancing V and $\mathcal{G}$ of a strictly resonant cavity by either modifying the magnetic field or using dielectrics, [22] and [23, 30]. However, our dielectric haloscope would be a poor resonator, compensating a relatively low $Q_{\rm d}$ with a huge V. This has completely different engineering challenges than an intermediate volume, high-Q cavity.

Large V resonators are typically more complicated mechanically, which implies longer tuning times. For high-Q cavities, as V increases modes tend to clutter [31] and it becomes increasingly difficult to identify and tune to them. Mode crossings become more frequent, with concomitant forbidden frequencies. Furthermore, for a large V resonant cavity the coupling of the output port needs to increase locally to compensate for a longer time-of-flight of photons in the cavity, leading to stronger mode distortions.

In our case, we have the flexibility to compensate for longer tuning times by using broadband and non-resonant configurations. Further, we avoid mode crossings by not having modes, rather quasi-modes with very broad widths. Lastly, by making the system as 1D as possible with a large A, and extracting the signal homogeneously across the last dielectric layer, we minimise any distortion caused by a local coupling to the detector. This allows us to avoid some of the issues of large V resonators.

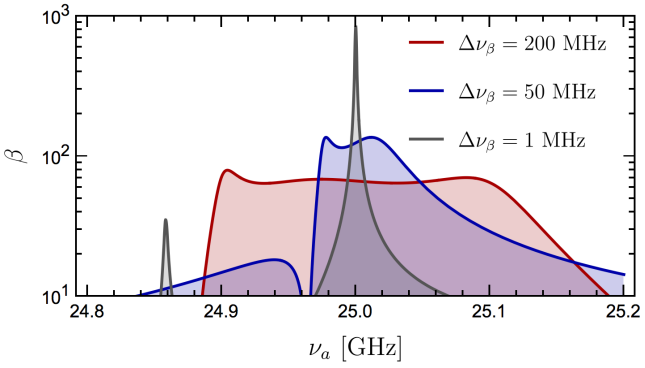

FIG. 2. Boost factor $\beta(\nu_a)$ for configurations optimised for $\Delta\nu_\beta = 200$, 50 and 1 MHz (red, blue and grey) centred on 25 GHz using a mirror and 20 dielectric disks ($d = 1$ mm, $\epsilon = 25$).

PROPERTIES OF THE BOOST FACTOR

Once we choose our dielectrics, fixing ϵ and d, the disk spacings remain as the only free parameters, giving us considerable control over the frequency response. Ideally, we would have two types of configurations, one providing a flat response so that a single configuration can measure a large frequency range simultaneously, and another with a larger β over a narrow band to discard statistical fluctuations and do precision axion physics in case of a discovery. We can numerically generate configurations that approach such responses.

One can predict the general behaviour of β by using the "Area Law": $\int \beta^2 d\nu_a$ is proportional to the sum over interfaces, which holds exactly when integrating over $0 \leq \nu_a \leq \infty$, and is a good approximation for frequency ranges containing the main peak [28]. According to the Area Law, an increase in the number of dielectrics gives a linear increase in $\int \beta^2 d\nu_a$. For a single set of dielectrics $\int \beta^2 d\nu_a$ is constant; one can trade width for power and vice versa, but cannot gain in both.

Figure 2 depicts $\beta(\nu_a)$ for a dielectric haloscope consisting of a mirror and 20 disks ($d = 1$ mm, $\epsilon = 25$). Spacings have been selected to maximise $\beta_{\rm min}$ within $\Delta\nu_\beta = 1$, 50 and 200 MHz centred on 25 GHz (our benchmark frequency corresponding to $m_a = 103.1\,\mu$eV). Figure 2 illustrates the Area Law: as we vary the bandwidth, the power changes by roughly the same factor. While the area is conserved, how efficiently it is used determines $\beta_{\rm min}$: flat responses are more efficient than narrow resonances, which are approximately Lorentzian. Using the Area Law we extrapolate to the 80 disk setup de-

scribed below: $\beta_{\rm min} \sim 275$ across 50 MHz should be possible. The achievable $\beta_{\rm min}$ changes with the optical thickness of a disk – in the example shown $\delta \sim 0.8\pi$, neither transparent nor fully reflective. Note that for a given d, there are frequency bands around $\nu_a = 1, 3, 5, ... \times \pi/\sqrt{\epsilon}d$ for which the dielectrics are transparent and β is limited to the sum of the EM waves $\beta_{\rm min} \leq 2N + 1$, where N is the number of disks. Further, at $\nu_a = 2, 4, 6, ... \times \pi/\sqrt{\epsilon}d$ the disks do not emit any radiation. Thus when large β or flexibility is required one must avoid these frequencies with a different set of dielectrics.

SETUP

Dielectrics with large ϵ enhance emission and resonance effects, leading to a higher β. A good candidate could be $LaAlO_3$ ($\epsilon \sim 25, \mu \sim 1$), which has a very small loss tangent $\sim 10^{-5}$ at low temperature. The transverse area is limited by the feasibility and cost of an intense magnet: apertures larger than one square meter are extremely challenging. Dielectric disks of that area would be made by tiling smaller pieces and could be repositioned using precision motors. The precision required can be estimated by studying the analytically tractable cases – the single cavity and the $\lambda_a/2$ symmetric case [26]. For Gaussian positioning errors, we require a standard deviation [28]

$$\sigma \ll 200\,\mu{\rm m} \left(\frac{10^2}{\beta}\right)^{1/2} \left(\frac{100\,\mu{\rm eV}}{m_a}\right). \qquad (8)$$

For example, for $\beta \sim 10^3$, $\sigma \ll 60\,\mu$m would be needed for $m_a = 100\,\mu$eV, though the exact sensitivity depends on the configuration. Thus it will probably be more practical to use a broadband search technique, scanning a larger mass range in each longer measurement. We are investigating this requirement with a prototype setup using 20 cm diameter Al_2O_3 disks. Comparisons of the simulated and measured transmissivity and reflectivity (which are correlated with β) indicate that few μm precision could be achieved. Diffraction appears to be negligible for the setup, but full numerical studies are required.

Thermal emission of the disks and mirror contributes to the noise of the experiment, but is suppressed when compared to a black body by both small dielectric losses and a good reflectivity, respectively. However, the haloscope will reflect thermal emission from the detector into itself. This can be reduced by cooling the detector to cryogenic temperatures. As detector, we would use a broadband corrugated horn coupled to a linear amplifier like state-of-the-art HEMT for its broadband capabilities (operable up to 40 GHz) and/or quantum limited amplifiers. Using a HEMT detector at room temperature we measured a 10^{-21} W signal at 17 GHz at 6 sigma in a one week run – we expect 100 times better performance at cryogenic temperatures. With $\beta \sim 400$ we would be sensitive to QCD axions.

DISCOVERY POTENTIAL

For a practical experiment one must scan across m_a. The procedure consists of arranging the dielectrics to achieve a roughly constant β in a region $\Delta\nu_\beta$, measuring for some time Δt, and readjusting the distances to measure an adjacent frequency range. The required β for a reasonably short Δt is given by Dicke's radiometer equation for the desired signal to noise ratio, $S/N = (P/T_{\rm sys})\sqrt{\Delta t/\Delta\nu_a}$, where the system noise temperature is $T_{\rm sys}$ and the axion line width $\Delta\nu_a \sim 10^{-6}\nu_a$. Collecting the signal with efficiency η, we get

$$\frac{\Delta t}{1.3\,{\rm days}} \sim \left(\frac{\rm S/N}{5}\right)^2 \left(\frac{400}{\beta}\right)^4 \left(\frac{\rm m^2}{A}\right)^2 \left(\frac{m_a}{100\ \mu{\rm eV}}\right) \times \left(\frac{T_{\rm sys}}{8\,{\rm K}}\right)^2 \left(\frac{10\,{\rm T}}{B_{\rm e}}\right)^4 \left(\frac{0.8}{\eta}\right)^2 C_{a\gamma}^4\,. \qquad (9)$$

In a single measurement we simultaneously search $\Delta\nu_\beta/\Delta\nu_a$ possible axion "channels". Thus the time to scan a given frequency range scales inversely to $\beta^4\Delta\nu_\beta$. As the Area Law implies that $\beta^2\Delta\nu_\beta$ is approximately conserved, it appears that narrow resonant peaks are optimal, as with conventional cavity haloscopes.

However, both the required placement precision and the time $t_{\rm R}$ needed to reposition the disks limit β. With 80 disks to be adjusted, $t_{\rm R}$ will be non-negligible – for an optimal scanning rate the measurement and readjustment times must be similar. At low m_a the β required to reach a given $|C_{a\gamma}|$ is relatively small, so the dielectric haloscope could be adjusted to scan a wider mass range simultaneously, moving to higher β at higher masses. If a potential signal is found, the dielectric haloscope could be reconfigured to enhance β at that frequency, quickly confirming or rejecting it at high significance.

In Fig. 3 we show the discovery potential of an 80 disk experiment with a run time of three years, by extrapolating from our 25 GHz solutions using the Area Law. We have used $A = 1\,{\rm m}^2$, $\epsilon = 25$, and $B = 10\,{\rm T}$. We assume 80% detection efficiency, quantum limited detection ($T_{\rm sys} \sim m_a$) and a conservative $t_{\rm R} = 1\,{\rm day}$. We give two examples, reaching $|C_{a,\gamma}| = 1, 0.75$ (light blue, dark blue). Similar results can be achieved by using a two stage process. A five year run with commercially available HEMT amplifiers with $T_{\rm sys} = 8\,{\rm K}$ would cover the low-mass range, for example $m_a \lesssim 120\,\mu$eV with $|C_{a\gamma}| = 1$. The high-mass range $m_a \lesssim 230\,\mu$eV shown in Fig. 3 would require another two years with a quantum limited detector. Adding disks and extending the run time could expand the search to $m_a \lesssim 400\,\mu$eV.

Our haloscope would cover a large fraction of the high-mass QCD axion parameter space with sensitivity to

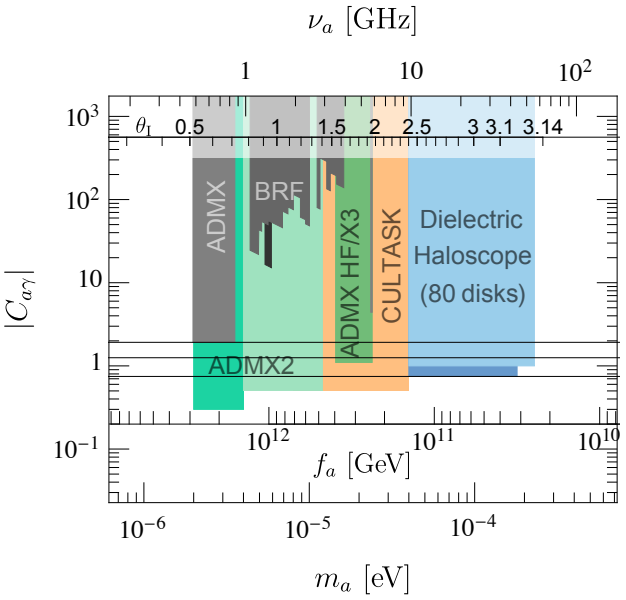

FIG. 3. Two examples of the discovery potential (light and dark blue) of our dielectric haloscope using 80 disks ($\epsilon = 25$, $A = 1\,\mathrm{m}^2$, $B_\mathrm{e} = 10\,\mathrm{T}$, $\eta = 0.8$, $t_\mathrm{R} = 1\,\mathrm{day}$) with quantum limited detection in a 3-year campaign. We also show exclusion limits (gray) and sensitivities (coloured) of current and planned cavity haloscopes [14, 15, 32–36]. The upper inset shows the initial angle θ_I required in Scenario A [37]. The lower inset depicts the f_a value corresponding to a given m_a, and the three black lines denote $|C_{a\gamma}| = 1.92, 1.25, 0.746$. Note that Scenario B predicts $50\,\mu\mathrm{eV} \lesssim m_a \lesssim 200\,\mu\mathrm{eV}$ [10, 38].

$|C_{a\gamma}| \sim 1$. In Scenario A, these masses correspond to large, but still natural, initial angles $2.4 \lesssim \theta_\mathrm{I} \lesssim 3.12$ [37]. Scenario B, our main goal, would be covered including the theoretical uncertainty in m_a (50–200 μeV [10, 38]) for KSVZ-type models with short-lived domain walls ($\mathcal{N} = 1$). Prime examples include the recent SMASH$_{d,u}$ models ($\mathcal{E} = 2/3, 8/3$) [38]. Models with $\mathcal{N} > 1$ require $m_a \gtrsim$ meV [10, 39], beyond our mass range. However, with some exceptions [40] they generally require a tuned explicit breaking of the PQ symmetry to avoid a domain-wall dominated universe [41].

CONCLUSION

In this Letter we have proposed a new method to search for high-mass (40–400 μeV) axions by using a mirror and multiple dielectric disks contained in a magnetic field – a dielectric haloscope. The key features are a large transverse area and the flexibility to use both broadband and narrow-band search strategies. With 80 disks one could search a large fraction of this high-mass range with sensitivity to the QCD axion.

ACKNOWLEDGMENTS

We acknowledge partial support by the Deutsche Forschungsgemeinschaft through Grant No. EXC 153 (Excellence Cluster "Universe"), the Alexander von Humboldt Foundation, as well as the European Commission under ERC Advanced Grant 339169 and under the Initial Training Network "Elusives" Grant No. H2020-MSCA-ITN-2015/674896. Part of this work was performed at the Bethe Forum "Axions" (7–18 March 2016), Bethe Center for Theoretical Physics, University of Bonn, Germany.

[1] R. D. Peccei, The strong CP problem and axions, Lect. Notes Phys. **741** 3 (2008) [arXiv:0607268].
[2] J. E. Kim and G. Carosi, Axions and the strong CP problem, Rev. Mod. Phys. **82**, 557 (2010) [arXiv:0807.3125].
[3] K. A. Olive *et al.* (Particle Data Group Collaboration), Review of particle physics, Chin. Phys. C **38**, 090001 (2014).
[4] C. A. Baker *et al.*, An improved experimental limit on the electric dipole moment of the neutron, Phys. Rev. Lett. **97**, 131801 (2006) [arXiv:0602020].
[5] J. Preskill, M. B. Wise and F. Wilczek, Cosmology of the invisible axion, Phys. Lett. B **120**, 127 (1983).
[6] L. F. Abbott and P. Sikivie, A cosmological bound on the invisible axion, Phys. Lett. B **120**, 133 (1983).
[7] M. Dine and W. Fischler, The not so harmless axion, Phys. Lett. B **120**, 137 (1983).
[8] G. G. Raffelt, Astrophysical axion bounds, Lect. Notes Phys. **741**, 51 (2008) [hep-ph/0611350].
[9] T. Hiramatsu, M. Kawasaki, K. Saikawa and T. Sekiguchi, Production of dark matter axions from collapse of string-wall systems, Phys. Rev. D **85** (2012) 105020; Erratum *ibid.* **86**, 089902 (2012) [arXiv:1202.5851].
[10] M. Kawasaki, K. Saikawa and T. Sekiguchi, Axion dark matter from topological defects, Phys. Rev. D **91**, 065014 (2015) [arXiv:1412.0789].
[11] L. Fleury and G. D. Moore, Axion dark matter: strings and their cores, JCAP **1601**, 004 (2016) [arXiv:1509.00026].
[12] P. Sikivie, Experimental tests of the invisible axion Phys. Rev. Lett. **51**, 1415 (1983); Erratum *ibid.* **52**, 695 (1984).
[13] G. Rybka (ADMX Collaboration), Direct detection searches for axion dark matter, Phys. Dark Univ. **4**, 14 (2014).
[14] B. M. Brubaker *et al.*, First results from a microwave cavity axion search at 24 micro-eV, arXiv:1610.02580.
[15] W. Chung, Launching axion experiment at CAPP/IBS in Korea, in *Proceedings of the 12th Patras Workshop on Axions, WIMPs and WISPs, Jeju, Korea* (2016), in preparation.
[16] D. Budker, P. W. Graham, M. Ledbetter, S. Rajendran and A. Sushkov, Proposal for a Cosmic Axion Spin Precession Experiment (CASPEr), Phys. Rev. X **4**, 021030 (2014) [arXiv:1306.6089].

[17] P. Sikivie, N. Sullivan and D. B. Tanner, Proposal for axion dark matter detection using an LC Circuit, Phys. Rev. Lett. **112**, 131301 (2014) [arXiv:1310.8545].

[18] Y. Kahn, B. R. Safdi and J. Thaler, Broadband and resonant approaches to axion dark matter detection, arXiv:1602.01086.

[19] A. Arvanitaki and A. A. Geraci, Resonantly detecting axion-mediated forces with nuclear magnetic resonance, Phys. Rev. Lett. **113**, 161801 (2014) [arXiv:1403.1290].

[20] P. Sikivie, Dark matter axions, Int. J. Mod. Phys. A **25**, 554 (2010) [arXiv:0909.0949].

[21] M. Kawasaki and K. Nakayama, Axions: theory and cosmological role, Ann. Rev. Nucl. Part. Sci. **63**, 69 (2013) [arXiv:1301.1123].

[22] G. Rybka, A. Wagner, A. Brill, K. Ramos, R. Percival and K. Patel, Search for dark matter axions with the Orpheus experiment, Phys. Rev. D **91**, 011701 (2015) [arXiv:1403.3121].

[23] D. E. Morris, An Electromagnetic Detector For Relic Axions, LBL-17915 (1984).

[24] S. K. Lamoreaux, K. A. van Bibber, K. W. Lehnert and G. Carosi, Analysis of single-photon and linear amplifier detectors for microwave cavity dark matter axion searches, Phys. Rev. D **88**, 035020 (2013) [arXiv:1306.3591].

[25] D. Horns, J. Jaeckel, A. Lindner, A. Lobanov, J. Redondo and A. Ringwald, Searching for WISPy cold dark matter with a dish antenna, JCAP **1304**, 016 (2013) [arXiv:1212.2970].

[26] J. Jaeckel and J. Redondo, Resonant to broadband searches for cold dark matter consisting of weakly interacting slim particles, Phys. Rev. D **88**, 115002 (2013) [arXiv:1308.1103].

[27] G. Grilli di Cortona, E. Hardy, J. P. Vega and G. Villadoro, The QCD axion, precisely, JHEP **1601**, 034 (2016) [arXiv:1511.02867].

[28] A. Millar, G. Raffelt, J. Redondo and F. Steffen, Dielectric haloscopes: theoretical foundations, MPP-2016-329, in preparation.

[29] P. Sikivie, Detection rates for 'invisible' axion searches, Phys. Rev. D **32**, 2988 (1985); Erratum *ibid.* **36**, 974 (1987).

[30] G. Rybka, Commissioning of the ADMX Gen 2 dark matter search in *Proceedings of the 12th Patras Workshop on Axions, WIMPs and WISPs, Jeju, Korea* (2016), in preparation.

[31] O. K. Baker *et al.*, Prospects for searching axion-like particle dark matter with dipole, toroidal and wiggler magnets, Phys. Rev. D **85**, 035018 (2012) [arXiv:1110.2180].

[32] S. J. Asztalos *et al.* (ADMX Collaboration), A SQUID-based microwave cavity search for dark-matter axions, Phys. Rev. Lett. **104**, 041301 (2010) [arXiv:0910.5914].

[33] C. Hagmann, P. Sikivie, N. S. Sullivan and D. B. Tanner, Results from a search for cosmic axions, Phys. Rev. D **42**, 1297 (1990).

[34] W. Wuensch *et al.*, Results of a laboratory search for cosmic axions and other weakly coupled light particles, Phys. Rev. D **40**, 3153 (1989).

[35] G. Carosi, Cavity-based searches for relic axions, *Talk given at Bethe Forum on Axions and the Low Energy Frontier* (2016), http://bctp.uni-bonn.de/bethe-forum/2016/axions/talks/Carosi.pdf

[36] K. van Bibber, Status of the ADMX-HF experiment, in *Proceedings of the 11th Patras Workshop on Axions, WIMPs and WISPs, Zaragoza, Spain* (2015),

[37] S. Borsanyi *et al.*, Lattice QCD for cosmology, arXiv:1606.07494.

[38] G. Ballesteros, J. Redondo, A. Ringwald and C. Tamarit, Unifying inflation with the axion, dark matter, baryogenesis and the seesaw mechanism, arXiv:1608.05414.

[39] A. Ringwald and K. Saikawa, Axion dark matter in the post-inflationary Peccei-Quinn symmetry breaking scenario, Phys. Rev. D **93**, 085031 (2016); Addendum *ibid.* **94**, 049908 (2016) [arXiv:1512.06436].

[40] G. Lazarides and Q. Shafi, Axion models with no domain wall problem, Phys. Lett. B **115**, 21 (1982).

[41] P. Sikivie, Of axions, domain walls and the early universe, Phys. Rev. Lett. **48**, 1156 (1982).